PHYSICAL REVIEW B VOLUME 40, NUMBER 12 15 OCTOBER 1989-II

Pressure dependence of phonon modes in GaAs/AlAs superlattices

P. Seguy and J. C. Maan
Max-Planck-Institut für Festkörperforschung, Hochfeld-Magnetlabor, B.P. 166X, F-38042 Grenoble, France

G. Martinez
Service National des Champs Intenses, Centre National de la Recherche Scientifique, B.P. 166X, F-38042 Grenoble, France

K. Ploog
Max-Planck-Institut für Festkörperforschung, 7000 Stuttgart 80, Federal Republic of Germany

(Received 1 May 1989)

Brillouin- and Raman-scattering measurements on a GaAs-AlAs superlattice have been performed as a function of the hydrostatic pressure up to 160 kbar. Below 110 kbar the acoustic folded and optical confined phonons have been measured, and the results are compared to the predictions of the actual models. Beyond 110 kbar the AlAs layers undergo a phase transition which is analyzed and discussed in comparison to previous results.

I. INTRODUCTION

The periodic spatial modulation in man-made semiconductor structures such as superlattices gives rise to original electronic and vibrational properties that have been extensively studied both theoretically and experimentally.[1]

In particular, in the past ten years, a lot of work has been devoted to the vibrational phenomena that occur in the GaAs/AlAs system;[2–8] besides the existence of interface modes,[7] it has been shown that the basic new features for phonons propagating along the growth direction of such structures can be described in terms of folded phonons (acoustical modes) and confined phonons (optical modes). The superperiodicity D of the superlattice (SL) is known to give rise to a folding of the acoustical-phonon dispersion curve in the SL reduced Brillouin zone; this leads to possible light scattering by doublets of phonons.[3,4] Within a continuous medium approximation, these doublets, labeled $i=1,2,\ldots$, are equidistant and their mean energy is given by

$$\bar{\omega}_i=2\pi i v_s/D \ , \tag{1}$$

v_s being the average sound velocity of the medium which for longitudinal vibrations is given by[3]

$$v_s=D\left[\frac{d_{\mathrm{GaAs}}}{(C_{11}^{\mathrm{GaAs}}/\rho_{\mathrm{GaAs}})^{1/2}}+\frac{d_{\mathrm{AlAs}}}{(C_{11}^{\mathrm{AlAs}}/\rho_{\mathrm{AlAs}})^{1/2}}\right]^{-1} , \tag{2}$$

d, C_{11}, and ρ being the layer width, the stiffness constant, and the density of the related materials, respectively.

In the case of optical vibrations, no propagating modes along the growth direction of the SL can be observed because the GaAs and AlAs optical-phonon density of states do not overlap. This leads to GaAs-like and AlAs-like confined phonons vibrating in the GaAs and AlAs layers, respectively. It has been pointed out that the energies of these confined modes sample the optical dispersion curve of the related material at wave-vector values equal[6] to $[2\pi/(n+1)a_0]m$, m labeling the related confined mode and $n(a_0/2)$ being the width of the confining layer composed of n monolayers.

However, though already intensively studied at ambient pressure, there is no report on the pressure dependence of all these modes and the purpose of this paper is to present the results of such a new investigation. We have therefore performed Raman and Brillouin experiments on a GaAs/AlAs superlattice as a function of pressure up to 150 kbar. The purpose of this new investigation was to check the basic concepts developed up to now to explain both acoustic folded and optical confined phonons. In addition, if such concepts are verified, we expect to have a direct information on the variation of the dispersion relation of the longitudinal-optical (LO) branch with pressure. Such information can normally only be obtained from neutron-diffraction experiments performed under pressure and involve a much more sophisticated experimental investigation than the one presented here.

A brief description of the experimental setup is given in Sec. II. Since in the range of pressure studied here (up to 150 kbar) the superlattice undergoes a phase transition,[9,10] we first present and discuss in Sec. III the experimental results on folded longitudinal-acoustical (LA) doublets as well as on GaAs-like and AlAs-like LO modes as a function of pressure up to 100 kbar. Section IV is devoted to the Raman investigation of the phase transition in the superlattice itself.

II. EXPERIMENTAL PROCEDURE

We have studied a 30-period GaAs(2 nm)/AlAs(6 nm) superlattice grown along the [100] direction by molecular-beam epitaxy on a GaAs substrate. The substrate was polished mechanically and the thickness of the sample reduced to 25 μm. Small pieces were cleaved with typical sizes of $80 \times 80\ \mu m^2$. The comparison of the optical spectra before and after the polishing process did not reveal any significant differences.

High pressures were obtained using the diamond-anvil-cell technique. A piece of sample was immersed in a methanol-ethanol mixture together with chips of rubis, used to calibrate the pressure. This system allows one to perform optical experiments (Raman and Brillouin scattering) in a backscattering geometry, and pressures up to 200 kbar can be reached. It was found that for pressures lower than 90 kbar, the hydrostaticity was better than 1%.

All the Brillouin data were obtained at room temperature in the $X(YZ)\bar{X}$ geometry. The 514.5-nm line of an Ar^+ laser was focused on the (100) surface of the superlattice, and the backscattered light was collected and analyzed using a Dilor RTI 30 Triple additive monochromator and detected by a GaAs-photocathode photomultiplier operating in a photon-counting mode. This apparatus was operating with a spectral resolution of about $0.9\ cm^{-1}$.

The Raman spectra were obtained at liquid-nitrogen temperature in a backscattering configuration. We used the standard 514.5- and 488.0-nm lines of an Ar^+ laser focused on the sample surface with a cylindrical lens in order to avoid heating. The backscattered light was analyzed by an OMARS 89 spectrometer composed of a double-substractive grating spectrometer (low-dispersion mode) or a double-additive grating spectrometer (high-dispersion mode), followed by a spectrograph with a cooled multichannel detection system. This apparatus has a maximal resolution of about $3.0\ cm^{-1}$ in the low-dispersion and $1.0\ cm^{-1}$ in the high-dispersion mode.

III. EXPERIMENTAL RESULTS UP TO 100 kbar

A. Acoustical modes

Figure 1 shows Brillouin spectra obtained in the $X(YZ)\bar{X}$ configuration at room temperature for two different pressures: at 1 bar we observe three equidistant doublets of folded LA phonons in accordance with previous reported results.[3,4] At higher pressures, the two first doublets can be followed up to 100 kbar and they are found to shift to higher energies as the pressure is increased. The increasing background on the low-energy side of the spectra is the remaining contribution of the elastic line.

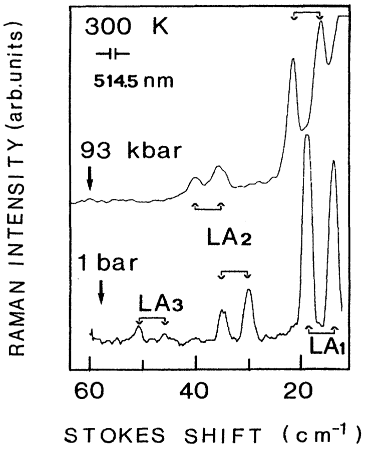

FIG. 1. Brillouin spectra taken in the $X(YZ)\bar{X}$ scattering configuration showing the behavior of the folded LA doublets under pressure.

Figure 2 shows the mean energy of these two doublets versus pressure: doublet $i=1$ (open circles) and doublet $i=2$ (solid circles). Within experimental error, the shift of these phonons is linear with pressure up to 100 kbar and has a slope as a function of the pressure for the second doublet which is twice as great as that of the first. This behavior can be well understood using the continuous-medium model and reflects mainly the increase of the elastic constant of the medium under pressure. Using Eqs. (1) and (2), it is possible to calculate the pressure dependence of each folded doublet versus the stiffness constant C_{11}, its pressure derivative dC_{11}/dP, and the bulk modulus B of the two materials constituting the superlattice. Table I lists the data concerning the elastic constants of the related compounds and their dependence on pressure. Since these numbers are the same within 3–5 %, we will use in the following the GaAs values for both of them.

Within this approximation we obtain for a doublet labeled i

$$\frac{d\omega_i}{dP}=\frac{\omega_i}{2C_{11}}\left[\frac{dC_{11}}{dP}-\frac{C_{11}}{3B}\right] . \tag{3}$$

The reduced first-order variation of this doublet is

$$\frac{\omega_i(P)-\omega_i(0)}{i}=P\frac{\omega_1(0)}{2C_{11}}\left[\frac{dC_{11}}{dP}-\frac{C_{11}}{3B}\right] , \tag{4}$$

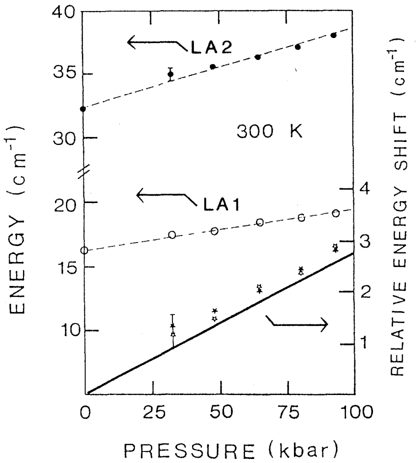

FIG. 2. Average energies of the doublets LA_1 and LA_2 (left scale) as a function of pressure. Dotted lines are guides for the eye. The reduced energy shifts of the first (open stars) as well as the second doublet (solid stars) are compared with the result of calculations (solid line).

TABLE I. Values of the different parameters used for GaAs and AlAs: the density (ρ), the lattice parameter (a_0), the stiffness constant (C_{11}) and its pressure derivative (dC_{11}/dP), and the isothermal bulk modulus (B_T) and its pressure derivative (dB_T/dP).

	GaAs	AlAs
ρ (g/cm^3)	5.317[a]	3.7[a]
a_0 (Å)	5.6535[a]	5.66[a]
C_{11} (dyn/cm^2)	11.81×10^{11}[a]	12.5×10^{11}[a]
dC_{11}/dP	4.63[a]	
B_T (10^{11} dyn/cm^2)	7.4[a] 7.6[d]	7.7[e]
dB_T/dP	4.67[a]	

[a] Experimental values at 300 K from Ref. 17.
[b] Calculated value from Ref. 17.
[c] Experimental value from Ref. 11.
[d] Estimated value at 80 K from Ref. 17.
[e] Calculated value from Ref. 11.

and is therefore independent of the folding order i. In Eq. (4), $\omega_1(0)$ is the mean energy of the first doublet at 1 bar.

The experimental reduced relative frequency shifts are represented in Fig. 2 for the first folded doublet $i=1$ (open stars) and the second doublet $i=2$ (solid stars). They are compared to the theoretical variation calculated using Eq. (4) (solid line in Fig. 2).

The agreement with the simple model we have used is very good and shows the validity of the continuous-medium model to describe these long-wavelength acoustical modes and their variation under pressure.

B. Optical modes

1. General behavior under pressure

Figure 3 shows Raman spectra obtained at low temperature in the backscattering configuration $X(YZ)\bar{X}$ (X being the growth direction of the superlattice) allowing us to see longitudinal-optical modes with B_2 symmetry. These data were recorded as a function of pressure up to 100 kbar with the 514.5-nm exciting line in the low-dispersion mode. At 1 bar, we observe two main structures at about 295 and 400 cm^{-1} which correspond to the GaAs- and AlAs-like optical modes of the superlattice, respectively.

Upon increasing pressure, these two structures are shifted towards higher energies corresponding to a positive pressure coefficient of these modes as expected for the LO vibrations of the related materials. A quantitative analysis of this variation will be detailed in the following. The second point which has to be noticed, is the variation of the relative intensity of the GaAs- and AlAs-like structures versus pressure: this corresponds to pressure-induced resonance phenomena which will be discussed later.

Let us first focus our attention on the spectral dependence of these phonon modes.

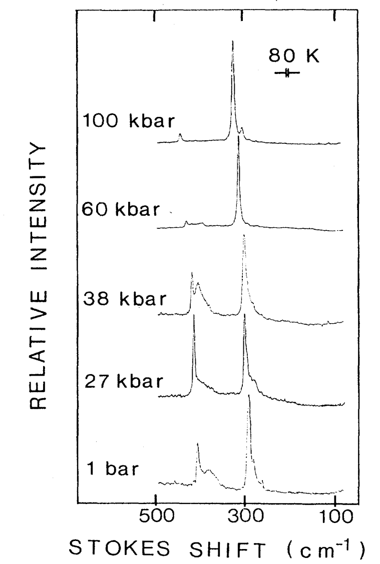

FIG. 3. Optical-phonon Raman spectra in the $X(YZ)\bar{X}$ configuration obtained with the 514.5-nm exciting line for different pressures.

2. GaAs-like modes

The details of the previous Raman spectra in the region of the GaAs-like optical mode are shown in Fig. 4(a). The use of the high-dispersion mode here allows us to see well-defined confined GaAs LO modes.

All the spectra have been aligned with respect to the LO bulk mode of the GaAs substrate. The frequency of this mode is measured in the same experimental conditions for each pressure using the back side (substrate) of the sample. In the following the energy of this bulk LO mode is taken as a reference, and the difference between this energy and that of a given confined mode will be called "confinement energy" of the related mode.

At 1 bar, we observe three GaAs-like confined LO modes, LO$_1$, LO$_3$, and LO$_5$, in the $X(YZ)\bar{X}$ spectra (B_2-symmetry modes) and two A_1-symmetry modes, LO$_2$ and LO$_4$, in the $X(ZZ)\bar{X}$ configuration as previously reported by Sood *et al.*[5] As the pressure is increased, the relative intensity of the different confined modes changes, and in a range of pressures between 35 and 55 kbar, the mixing of the A_1 and B_2 symmetries of the modes appear in the $X(YZ)\bar{X}$ spectra. In particular, for pressures of about 45 kbar (see Fig. 4), the main peak in the $X(YZ)\bar{X}$ spectra corresponds to a B_2 component of the LO$_2$ confined mode which was a pure A_1 mode at low pressures. This situation develops for all confined modes for pressure between 60 and 75 kbar, and no difference is observed between the $X(YZ)\bar{X}$ and $X(ZZ)\bar{X}$ spectra as shown on the upper part of Fig. 5 at 72 kbar. At higher pressure, the spectra are dominated by the bulk-LO-mode contribution. This occurs because the pressure tunes the band gap of the superlattice above the energy of the 514.5-nm laser line (see Fig. 9).

Using a different exciting line (488.0 nm), a similar behavior is observed but shifted towards higher pressures

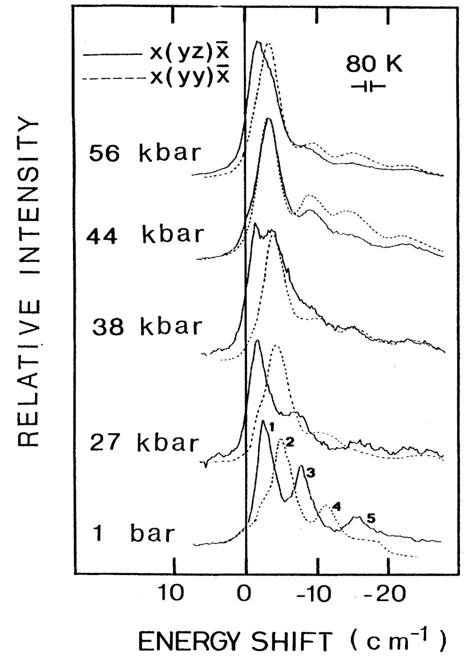

FIG. 4. High-resolution Raman spectra showing the variation of the GaAs-like confined mode under pressure. All the spectra, recorded with the 514.5-nm line, have been aligned with respect to the GaAs bulk LO mode (vertical line). The labeling of the confined modes is indicated in spectrum taken at 1 bar.

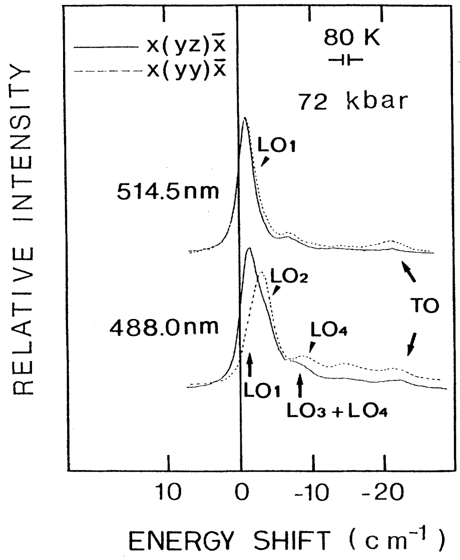

FIG. 5. High-resolution Raman spectra of the GaAs-like LO modes at pressure equal to 72 kbar with two different exciting laser lines. The origin of the energy scale is set to that of the GaAs bulk LO mode.

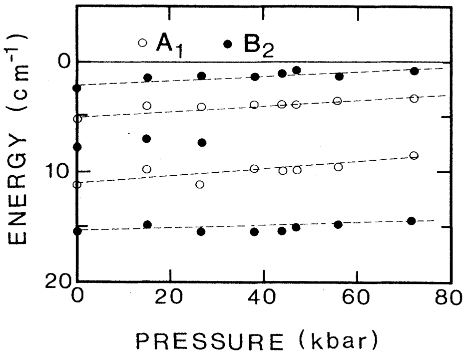

FIG. 6. Confinement energies of the GaAs-like confined LO modes as a function of pressure. The origin of the energy scale is that of the LO bulk mode of GaAs. Dotted lines are drawn to guide the eye.

(about 15 kbar) and the confined modes can be seen up to 72 kbar (Fig. 5). We attribute this behavior to a resonance phenomena and will discuss this point in Sec. III B 4. At higher pressures, the scattering from the substrate dominates in this frequency range, though the AlAs-like modes remain visible (Fig. 3).

Focusing on the dependence on the pressure of the energy of the maxima with respect to bulk GaAs, it is possible to measure the confinement energies of four confined modes up to 72 kbar as shown in Fig. 6. In general a small decrease of these relative energies is observed. As pointed out in the introduction, it is possible to use these data to reconstruct the LO dispersion curve of bulk GaAs in the [100] direction. The result of this procedure is shown in Fig. 7 for two different pressures. The noticeable flattening of the dispersion curve at high pressure corresponds to a change in the dispersion relation and, therefore, to a q wave-vector dependence of the pressure coefficient of the optical modes inside the Brillouin zone, i.e., the pressure coefficient of large-q LO phonons is

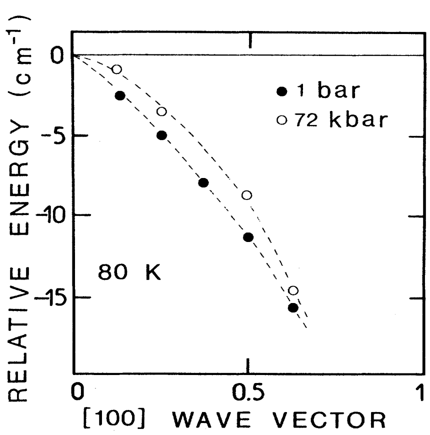

FIG. 7. The GaAs-LO dispersion curve along the [100] direction of the Brillouin zone as deduced from the experimental results for two different pressures.

larger than that of the zone-center LO bulk mode. This result is in qualitative agreement with previous calculations[12,13] on various zinc-blende ionic compounds which predict a pressure coefficient increasing with the wave vector along the [100] direction for each compound. However, to our knowledge, no calculation directly applicable to the case of GaAs exists.

3. *AlAs-like modes*

Figure 8 shows the behavior of the AlAs-like LO modes for different pressures using a high-dispersion mode. These spectra are obtained in the $X(YZ)\bar{X}$ scattering geometry. As expected, we have not resolved any AlAs confined phonons because of the large layer width of this material. In fact, AlAs-like confined LO modes have only been measured[8] for superlattices with AlAs layer width below 2.5 nm. The sharp peak we observe at 1 bar can therefore be considered as an AlAs-bulk mode. The small asymmetry on the low-energy side of this peak could be due to the contribution of the other levels of confined modes.

As the pressure is increased, this AlAs-like LO mode is shifted towards higher energy at a rate of about 0.44 cm^{-1}/kbar. A broad structure appears between the AlAs-LO and transverse optical (TO) energies in a range of pressure corresponding to the resonance of the A_1 GaAs-like LO modes. Such a phenomenon has already been observed in previous Raman investigations by Cardona *et al.*,[7] and this broad peak has been assigned to an AlAs-like interfacial mode.

4. *Resonant behavior and band structure*

Two main characteristic features that we attribute to resonant phenomena are observed in our experiments: (i) the A_1 GaAs-like lines increase in intensity and get some forbidden component in the $X(YZ)\bar{X}$ spectra, in a range of pressure between 35 and 55 kbar with the 514.5-nm exciting line and between 55 and 75 kbar with the 488.0-nm exciting line, respectively, and (ii) a similar intensity dependence versus pressure is observed for the AlAs-like interfacial mode.

These two characteristics have already been observed in previous Raman-scattering experiments on GaAs/AlAs superlattices[5] and have been explained as a resonant phenomenon dominated by the impurity-induced Fröhlich-interaction scattering mechanism occurring when the exciting energy of the laser line is tuned through the energy of the excitonic transition in the GaAs wells plus the energy of the related LO phonons (outgoing resonance energy).

In our experiment, for a given exciting line, the band gaps of the materials in the superlattice vary with pressure as shown in Fig. 9. The confined electronic levels in the GaAs wells increase with pressure roughly as does the Γ_6^c-Γ_8^v GaAs-bulk direct band gap.[14-16] The variation with pressure of the AlAs indirect band gaps has been assumed to be the same as the GaAs one.

We have measured the excitonic recombination in our sample at 1 bar to be at an energy $E=1.845$ eV that implies an outgoing resonance energy of $E+\hbar\omega_{\mathrm{LO}}=1.88$ eV; assuming the pressure coefficient of about 10 meV/kbar for the excitonic recombination[15,16] to be the same as that of the gap, the resonance energy matches 2.410 eV (514.5-nm laser line) at $P=53$ kbar and 2.54 eV (488.0-nm laser line) at $P=66$ kbar which is in good agreement with our measurements.

More surprising is the resonant phenomenon which occurs between 15 and 30 kbar for the LO mode of AlAs. The relative intensity of this mode with respect to the intensity of the main GaAs-like mode is found to increase

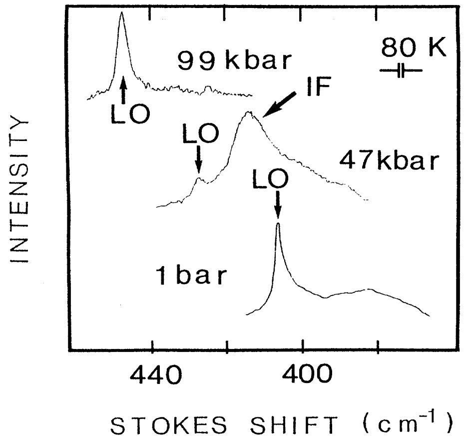

FIG. 8. High-resolution Raman spectra of the AlAs-like optical modes for three different pressures. Note the activation of the AlAs-interfacial mode (IF) under resonant conditions at 47 kbar.

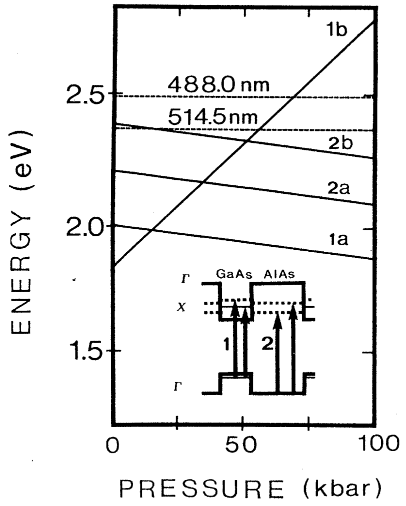

FIG. 9. Expected pressure dependence of the main electronic transitions in GaAs/AlAs superlattices. 1*a* refers to the transition between the heavy-hole valence band and the X_{6C} conduction band in the GaAs layers. The lower excitonic transition associated with the first confined electron and heavy-hole levels of the GaAs wells is labeled 1*b*; 2*a* and 2*b* refer, respectively, to the AlAs X_{6C}-Γ_{8V} and X_{7C}-Γ_{8V} indirect band gaps.

at low pressures and then to decrease for pressures higher than 27 kbar as shown in Fig. 3. Since no resonance phenomena are expected for the GaAs optical modes below 30 kbar, we assign this intensity variation to resonant phenomena originating from the absorption of light in the AlAs layers; this can be due to the tuning of the X_7^c-Γ_8^v indirect band gap of this material with the 514.5-nm exciting line when the pressure is increased, which indeed coincides with the 514.5-nm line energy at around 20 kbar as illustrated in Fig. 9.

IV. THE AlAs PHASE TRANSITION

Though the main purpose of this study was not to study the problem of the AlAs phase transition, we took the opportunity we had to investigate it with our techniques since, as reported by Weinstein *et al.*,[9] some anomalies have been previously observed for the dependence of the critical pressure P^c as a function of the AlAs thickness. To address this problem it is interesting to find an internal probe for the critical pressure applied to the sample: this can be the LO-phonon energy of GaAs.

In Fig. 10 are plotted the low-temperature (80 K) peak frequencies corresponding to the GaAs-LO bulk mode measured on the substrate (squares, right scale) and the AlAs-LO mode of the superlattice (dots, left scale) versus pressure (upper scale) and versus the relative lattice compression (lower linear scale). The lattice parameter a under compression is related to the pressure with Murnaghan's equation

$$P=(B/B')[(a_0/a)^{3B'}-1] ,$$

where a_0 is the lattice parameter at 1 bar and B' in the derivative of the bulk modulus B with respect to pressure. With this scaling, the observed LO-AlAs and -GaAs frequencies fall on a straight line within the experimental errors:

$$\omega_{\mathrm{LO}}^{\mathrm{GaAs}}=294+(975\pm15)(-\Delta a/a_0) ,$$

$$\omega_{\mathrm{LO}}^{\mathrm{AlAs}}=404.3+(1280\pm30)(-\Delta a/a_0) .$$

The related Grüneisen coefficients $\gamma=(1/3\omega_0)[\Delta\omega/(\Delta a/a_0)]$ are

$$\gamma_{\mathrm{LO}}^{\mathrm{GaAs}}=1.105\pm0.017 ,$$

$$\gamma_{\mathrm{LO}}^{\mathrm{AlAs}}=1.055\pm0.025 ,$$

at a temperature of 80 K.

These two values are very close to each other and reveal anharmonic properties which are similar for these two III-V compounds. The Grüneisen coefficient of the GaAs-LO mode at 80 K is found to be a little smaller than its room-temperature value ($\gamma_{300\,\mathrm{K}}=1.23\pm0.02$) which, as expected, reflects the decrease of anharmonicity in the medium as the temperature decreases.

The measurement of the GaAs-bulk mode was possible up to the maximum pressure we have reached, while that of AlAs was recorded only up to 112 kbar. At this pressure the sample, which had become transparent due to the increase of the GaAs band gap, initially becomes darker although still remains transparent. Upon increasing the pressure, the phase transition propagates further inside the sample until at some higher pressure the entire sample has become completely opaque. Such phenomena have been already observed for AlAs/GaAs superlattices[9] and correspond to a phase transition of the AlAs layers which transforms into a more closely packed structure.

Figure 11 shows the Raman spectra obtained in the $X(YZ)\bar{X}$ geometry with the 514.5-nm line: at 106 kbar (lower spectrum), the AlAs-LO mode is unambiguously seen as well as the GaAs-LO mode, which at this pressure arises mainly from the substrate as pointed out previously. At 112 kbar, some AlAs layers in the superlattice undergo a phase transition leading to a decrease of

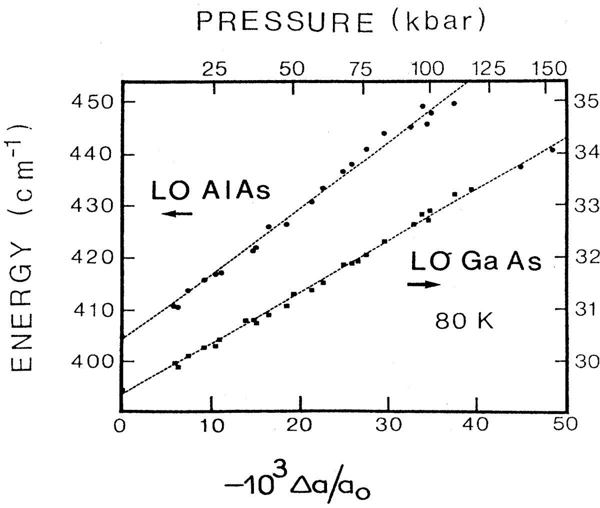

FIG. 10. AlAs and GaAs LO-phonon energies as a function of pressure (top scale) and of the relative lattice compression (lower scale).

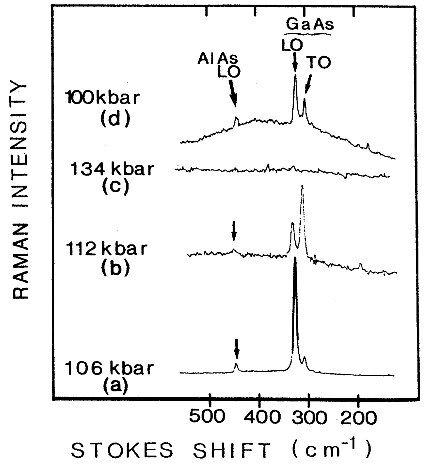

FIG. 11. Low-dispersion mode Raman spectra in the pressure range of the AlAs phase transition. (a) Before the phase transition. (b) Beginning of the phase transition. (c) After the phase transition. (d) After the reversal of the phase transition.

the penetration depth of the exciting line; the scattering from the untransformed AlAs layers can still be observed. The signal from GaAs is significantly decreased and the TO mode, which is normally forbidden in this scattering geometry, is found to dominate the spectra showing that very strong depolarization phenomena occur when the light passes through the transformed layers of the superlattice. At pressures higher than 120 kbar, the sample is completely opaque and the Raman signal disappears from the superlattice side as shown in the spectra taken at 134 kbar.

By lowering the pressure down to about 20 kbar it is possible to reverse the phase transition. The upper spectrum of Fig. 10 at 100 kbar has been recorded after such a cycle, and the AlAs-LO scattering can be seen clearly showing that the AlAs layers have been retransformed in their initial zinc-blende structure.

We must point out that, contrary to Weinstein's results,[9] we observe no superpressing phenomena for our 2-nm GaAs/6-nm AlAs superlattice; indeed, the phase transition is found to occur a little below the range of pressure reported for bulk AlAs (Ref. 9) ($P^c \simeq 123$ kbar). For free-standing epilayers of metalorganic chemical-vapor-deposition (MOCVD) grown superlattices with 2.5-nm GaAs and 6-nm AlAs layers, the pressure transition as reported in Ref. 9 was found to be 166±4 kbar; in our case, however, the substrate is not removed. We want to stress that a wrong calibration of the pressure (with the rubis scale) cannot be invoked, since, as can be seen in Fig. 10, one can use the variation of the bulk GaAs-LO mode as well to calibrate the actual pressure inside the sample and obtain the same results. This situation is very surprising since we would expect any superpressing phenomenon to be more probable in our case than in free-standing epilayers. We have no satisfactory explanation for these differences. We therefore estimate the pressure of the phase transition of AlAs ranging around 110 kbar and may be even lower since the first sign of the transition is already detected upon increasing pressure. This phase transition is reversible if the ultimate pressure reached is not too high; if it exceeds 160 kbar, the actual superlattice spectrum is no longer recovered at lower pressures.

V. CONCLUSION

We have reported on Brillouin- and Raman-scattering experiments performed on a GaAs-AlAs superlattice as a function of the pressure. Both acoustic folded and optical confined phonons have been observed up to 100 kbar and their variation as a function of the pressure can be explained well by the standard models. The variation with pressure of the dispersion relation of the GaAs-LO mode has been obtained, but remains to be reproduced theoretically on a basis of *ab initio* calculations.

The phase transition of the AlAs layers has been recorded and found to occur at a critical pressure not very different from that reported for bulk material, but significantly lower than that reported for a superlattice with similar parameters. This discrepancy is not actually understood and requires further experiments devoted to this particular aspect.

ACKNOWLEDGMENTS

The "Service National des Champs Intenses" is "Laboratoire associé à l'Université Joseph Fourier de Grenoble."

---

[1] *Heterojunctions and Semiconductor Superlattices, Proceedings of the Les Houches Winter School of Theoretical Physics, France, 1985,* edited by G. Allan, G. Bastard, N. Boccara, M. Larsmoo, and M. Voos (Springer-Verlag, Berlin, 1985).

[2] M. V. Klein, IEEE J. Quantum Electron. **QE-22**, 1760 (1986).

[3] C. Colvard, R. Merlin, M. V. Kein, and A. C. Gossard, Phys. Rev. Lett. **45**, 298 (1980).

[4] B. Jusserand, D. Paquet, A. Regreny, and J. Kervarec, Solid State Commun. **48**, 499 (1983).

[5] A. K. Sood, J. Menendez, M. Cardona, and K. Ploog, Phys. Rev. Lett. **54**, 2111 (1985).

[6] B. Jusserand and D. Paquet, Phys. Rev. Lett. **56**, 1752 (1986).

[7] A. K. Sood, J. Menendez, M. Cardona, and K. Ploog, Phys. Rev. Lett. **54**, 2115 (1985).

[8] Z. P. Wang, D. S. Jiang, and K. Ploog, Solid State Commun. **65**, 661 (1988).

[9] B. A. Weinstein, S. K. Hark, R. D. Burnham, and R. Martin, Phys. Rev. Lett. **58**, 781 (1987).

[10] B. A. Weinstein, S. K. Hark, and R. D. Burnham, in *Proceedings of the 18th International Conference on the Physics of Semiconductors, Stockholm, 1986,* edited by O. Engström (World Scientific, Singapore, 1987), p. 1253.

[11] P. K. Lam, M. L. Cohen, and G. Martinez, Phys. Rev. B **35**, 9190 (1987).

[12] C. Patel, W. F. Sherman, and G. R. Wilkinson, Phys. Status Solidi B **111**, 653 (1982).

[13] D. N. Talwar, M. Vandervyver, K. Kunc, and M. Zigone, Phys. Rev. B **24**, 741 (1981).

[14] U. Venkasteswaran, M. Chandrasekhar, H. R. Chandrasekhar, T. Wolfram, R. Fisher, W. T. Masselink, and H. Morkoç, Phys. Rev. B **31**, 4106 (1985).

[15] D. J. Wolford, in Ref. 10, p. 1115.

[16] P. Lefebvre, B. Gil, and H. Mathieu, Phys. Rev. B **35**, 5630 (1987).

[17] *Landolt-Börnstein, Numerical Data and Functional Relationships in Sciences and Technology* (Springer-Verlag, Berlin, 1982), Group 3, Vol. 17a.